Linear thermoacoustic instability in the time domain

S. Karpov and A. Prosperetti
Department of Mechanical Engineering, The Johns Hopkins University, Baltimore, Maryland 21218

(Received 30 April 1997; accepted for publication 17 February 1998)

An approximate time-domain description of the development of the thermoacoustic instability in gas-filled tubes is developed by exploiting the difference between the instability time scale and the period of standing waves. The perturbation results compare very favorably with the exact frequency-domain theory of Rott. The perturbation results are further simplified by introducing a short-stack approximation which is numerically much simpler and only slightly less accurate. An approximate expression for the critical temperature gradient accounting for viscous effects and other design features is also derived. In addition to the fundamental mode of a tube closed at both ends, the theory includes higher modes as well as open-end boundary conditions. © *1998 Acoustical Society of America.* [S0001-4966(98)00606-7]

PACS numbers: 43.35.Ud [HEB]

INTRODUCTION

The linear theory of thermoacoustic effects as developed in the well-known series of papers by Rott[1–4] (good reviews are provided by Wheatley[5] and Swift[6]) is based on a formulation in the frequency domain. In the present paper we develop an approximate time-domain approach that is valid when the period of standing waves is much shorter than the growth rate of the instability. Since this condition is commonly met in practice, we expect the present formulation to furnish a realistic description of the time evolution of the instability in a wide variety of situations.

One of the main results of the present work is an expression for the linear growth rate of the thermoacoustic instability or, below threshold, for the decay rate of standing waves. This latter result can also be viewed as expressing the power requirement for the operation of a thermoacoustic refrigerator. In the past these results have been approached by estimating the so-called work flux (see, e.g., Ref. 6) or Q-value of the device.[7–9] Our method may therefore be interpreted as a different approach to the evaluation of these quantities. Its advantage is a greater flexibility that enables us to considerably simplify their quantitative evaluation with respect to the exact theory of Rott while at the same time maintaining a greater accuracy than existing approximations.

A second result of the paper is an unambiguous definition of the concept of critical temperature gradient when viscous and thermal effects are both important and an accurate approximate expression for this quantity.

I. MATHEMATICAL MODEL

In Watanabe *et al.*[10] it was shown that a model of thermoacoustic devices that, in the frequency domain, is exactly equivalent to Rott's, may be written in the form

$$\frac{\partial \rho}{\partial t}+\frac{1}{S}\frac{\partial}{\partial x}(S\rho_0 u)=0, \tag{1}$$

$$\rho_0\frac{\partial u}{\partial t}+\frac{\partial p}{\partial x}=-\rho_0\mathscr{D}(u), \tag{2}$$

$$\frac{\partial p}{\partial t}+\frac{\gamma p_0}{S}\frac{\partial (Su)}{\partial x}=(\gamma-1)\left[\mathscr{H}(T_w-T)-\frac{dT_w}{dx}\mathscr{Q}(u)\right]. \tag{3}$$

The system of equations is closed by assuming the validity of the perfect gas law. Here ρ, p, T, and u are the density, pressure, temperature, and velocity fields. The spatial coordinate x is directed along the axis of the device, $S(x)$ is the (possibly variable) cross-sectional area, and γ the ratio of specific heats. The subscript zero denotes undisturbed quantities. The temperature $T_w(x)$ of the solid surfaces in contact with the gas (i.e., the tube walls and the stack plates) is assumed to be only a function of x and is taken to be prescribed in the following. It should be noted that, even when this quantity evolves with time, it does so only slowly (compared with the period of the oscillations) and therefore the present method can be extended to deal with this case as well as noted below.

The drag operator $\mathscr{D}$ and the heat transfer operators $\mathscr{H}$ and $\mathscr{Q}$ are given, in the frequency domain, by

$$\tilde{\mathscr{D}}(u)=i\omega\frac{f_V}{1-f_V}\tilde{u}, \tag{4}$$

$$\tilde{\mathscr{H}}(T_w-T)=-i\omega\rho_0 c_p\frac{f_K}{1-f_K}\tilde{T}', \tag{5}$$

$$\tilde{\mathscr{Q}}(u)=\rho_0 c_p\left[\frac{1}{1-\sigma}\left(\frac{1}{1-f_V}-\frac{\sigma}{1-f_K}\right)-1\right]\tilde{u}. \tag{6}$$

Here $T'=T-T_w$ and tildes denote frequency-domain quantities. The parameters $f_{V,K}$ depend on the ratio of the diffusion lengths $\delta_{V,K}$ to the plate spacing l and, for disturbances proportional to $\exp i\omega\hat{t}$, are given by[6]

$$f=(1-i)\frac{\delta}{l}\tanh(1+i)\frac{l}{2\delta}, \tag{7}$$

where the index can be V or K. The viscous and thermal penetration lengths $\delta_{V,K}$ are given by

 0001-4966/98/103(6)/3309/9/$10.00

$$\delta_V=\sqrt{\frac{2\nu}{\hat{\omega}}},\quad \delta_K=\sqrt{\frac{2\alpha}{\hat{\omega}}}=\frac{\delta_V}{\sqrt{\sigma}},\tag{8}$$

with ν the kinematic viscosity, σ the Prandtl number, and $\alpha=\nu/\sigma$ the thermal diffusivity. For a circular cross section with radius r_0 one has instead[1]

$$f=\frac{2J_1((i-1)(r_0/\delta))}{(i-1)(r_0/\delta)J_0((i-1)(r_0/\delta))},\tag{9}$$

again valid for both f_V and f_K. When the diffusion penetration depths are small compared with either l or r_0, f given by either (7) or (9) admits the asymptotic approximation

$$f\simeq(1-i)\,\frac{\delta}{l},\quad f\simeq(1-i)\,\frac{\delta}{r_0}.\tag{10}$$

More generally, for other cross section shapes, in this limit one may set $f\simeq 2(1-i)\delta/d_h$, where $d_h=4S(x)/s(x)$ is the hydraulic diameter defined in terms of the cross-sectional area S and the ''wetted'' perimeter s.

If Eqs. (1)–(3) are written in the frequency domain, after reduction to a single equation by differentiation and elimination, one recovers Rott's equation:

$$\frac{1}{S}\frac{d}{dx}\left[(1-f_V)S\,\frac{d\tilde{p}}{dx}\right]+\frac{1}{T_w}\frac{dT_w}{dx}\left(1+\frac{\sigma f_V-f_K}{1-\sigma}\right)\frac{d\tilde{p}}{dx}+\frac{\hat{\omega}^2}{c^2}\,[1+(\gamma-1)f_K]\tilde{p}=0.\tag{11}$$

The local adiabatic speed of sound $c(x)$ equals $\sqrt{\gamma RT_w(x)}$, with R the universal gas constant divided by the gas molecular mass, and is therefore also variable in general along the axis of the system.

II. THE STABILITY CALCULATION

Experiment (see, e.g., Refs. 5, 8) shows that the initial build-up of the thermoacoustic instability has the character of a modulated standing wave the frequency of which is essentially dictated by the resonator, while the amplitude is slowly varying in time. This observations suggests the possibility of setting up a perturbation scheme based on the smallness of the ratio of the characteristic period of oscillation to the characteristic time for the development of the instability.

In the framework of the previous model, the terms in the left-hand side of Eqs. (1)–(3) describe linear acoustic waves in a gas column with variable cross-sectional area and temperature stratification and are therefore responsible for the ''carrier'' frequency of the wave. The heart of the thermoacoustic effect is in the terms in the right-hand sides and, more specifically, in the right-hand side of the energy equation (3). The observed slowness of the modulation implies that these terms are small or, since $\mathscr{D}$, $\mathscr{H}$, and $\mathscr{Q}$ all vanish with $f_{V,K}$, that the f's are small. In order to set up a perturbation scheme, we take therefore $f_{V,K}$ to be of order $\epsilon\ll 1$ and we will treat the ratio $f_{V,K}/\epsilon$ as a quantity of order 1. While a formal definition of ϵ is not necessary as the final results do not explicitly depend on this parameter, according to (10), one may think of it as the ratio δ/l.

To proceed with a formal development of the previous observation, we introduce the scaled times

$$\hat{t}=t,\quad \tau=\epsilon t,\tag{12}$$

and, according to the method of multiple time scales, we treat $\hat{t}$ and τ as independent variables. The original variable t is recovered at the end of the calculation by using (12) (see, e.g., Refs. 11, 12). As a consequence of these definitions we have, correct to order ϵ,

$$\frac{\partial}{\partial t}=\frac{\partial}{\partial\hat{t}}+\epsilon\,\frac{\partial}{\partial\tau}.\tag{13}$$

We also expand the dependent variables p, u, etc., in a power series in ϵ; for example,

$$p=p_1+\epsilon p_2+\cdots,\tag{14}$$

with a similar notation for u, etc. Now these expansions are substituted into (1) to (3) where (13) is used to express the time derivative. Upon separating orders, to zero order in ϵ, we have

$$\frac{\partial\rho_1}{\partial\hat{t}}+\frac{1}{S}\frac{\partial}{\partial x}(S\rho_0u_1)=0,\tag{15}$$

$$\rho_0\,\frac{\partial u_1}{\partial\hat{t}}+\frac{\partial p_1}{\partial x}=0,\tag{16}$$

$$\frac{\partial p_1}{\partial\hat{t}}+\frac{\gamma p_0}{S}\,\frac{\partial(Su_1)}{\partial x}=0,\tag{17}$$

and, at the next order,

$$\frac{\partial\rho_2}{\partial\hat{t}}+\frac{1}{S}\frac{\partial}{\partial x}(S\rho_0u_2)=-\frac{\partial\rho_1}{\partial\tau},\tag{18}$$

$$\rho_0\,\frac{\partial u_2}{\partial\hat{t}}+\frac{\partial p_2}{\partial x}=-\frac{\partial u_1}{\partial\tau}-\frac{1}{\epsilon}\,\rho_0\mathscr{D}(u_1),\tag{19}$$

$$\frac{\partial p_2}{\partial\hat{t}}+\frac{\gamma p_0}{S}\,\frac{\partial(Su_2)}{\partial x}=-\frac{\partial p_1}{\partial\tau}-(\gamma-1)\times\left[\frac{1}{\epsilon}\,\mathscr{H}(T_1')+\frac{1}{\epsilon}\,\mathscr{Q}(u_1)\,\frac{dT_w}{dx}\right].\tag{20}$$

A. Zero order

The three equations (15) to (17) can be combined to give

$$\frac{1}{S}\frac{\partial}{\partial x}\left(c^2S\,\frac{\partial p_1}{\partial x}\right)-\frac{\partial^2p_1}{\partial\hat{t}^2}=0.\tag{21}$$

The solution of this equation may be taken in the form

$$p_1(x,\hat{t},\tau)=A(\tau)P_1(x)\exp(i\omega\hat{t})+\text{c.c.},\tag{22}$$

where c.c. denotes the complex conjugate, and the eigenfunction $P_1(x)$ and eigenfrequency ω are determined by solving the eigenvalue problem

$$\frac{1}{S}\frac{d}{dx}\left(c^2 S\frac{dP_1}{dx}\right)+\omega^2 P_1=0, \tag{23}$$

subject to appropriate boundary conditions. In this paper we only consider rigid or open terminations at the ends of the tube and therefore

$$\frac{dP_1}{dx}=0 \quad \text{or} \quad P_1=0 \quad \text{at} \quad x=0,\ x=L. \tag{24}$$

With these conditions, it can readily be shown by standard techniques that the eigenvalue ω is real (see, e.g., Refs. 14, 15). The eigenfunction P_1 can therefore also be taken real and, for later convenience, we normalize it so that

$$\int_0^L S(x)P_1^2(x)dx=Vp_0^2, \tag{25}$$

where V is the volume of the device and p_0 is the undisturbed static pressure. Since the total acoustic energy in the device, to the present approximation, is given by (see, e.g., Ref. 16 section 63)

$$\mathscr{E}=\int_0^L S(x)\frac{\langle p_1^2\rangle}{\rho_0 c^2}\,dx=\frac{A^2}{2\gamma p_0}\int_0^L S(x)P_1^2 dx=A^2\mathscr{E}_0, \tag{26}$$

we see that normalization (25) is equivalent to normalizing the energy by

$$\mathscr{E}_0=\frac{Vp_0}{2\gamma}. \tag{27}$$

It is readily found that u_1, ρ_1, and T_1' also satisfy Eq. (21) and therefore they can also be written in the form (22) with the same ω and proportionality to the same function $A(\tau)$. In particular, from (16),

$$U_1(x)=\frac{i}{\omega\rho_0}\frac{dP_1}{dx}. \tag{28}$$

B. First order

To order ϵ, the drag and heat transfer operators $\mathscr{D}$, $\mathscr{H}$, and $\mathscr{Q}$ operate on the variable $\hat{t}$ and, since the dependence on this variable is only through the exponential factor $\exp i\omega\hat{t}$, one can use the Fourier-space representation of these operators given in (4)–(6). Upon substitution of solution (22) for p_1 and similar expressions for the other first-order fields into (18)–(20), we thus find

$$\begin{aligned}\frac{1}{S}\frac{\partial}{\partial x}\left(c^2 S\frac{\partial p_2}{\partial x}\right)-\frac{\partial^2 p_2}{\partial\hat{t}^2}&=\left\{2i\omega\frac{dA}{d\tau}P_1-\frac{A}{\epsilon}\left[\frac{1}{S}\frac{\partial}{\partial x}\left(\frac{if_V}{1-f_V}\omega\rho_0 Sc^2U_1\right)\right.\right.\\&\quad+(\gamma-1)\omega^2 f_K P_1(x)\\&\quad\left.\left.-i\frac{f_V-f_K}{(1-\sigma)(1-f_V)}\gamma\frac{\omega p_0 U_1}{T_w}\frac{dT_w}{dx}\right]\right\}\exp i\omega\hat{t}+\text{c.c.}\end{aligned} \tag{29}$$

The forcing at frequencies $\pm\omega$ in the right-hand side will generate resonant terms proportional to $\hat{t}\exp i\omega\hat{t}$ in the solution for p_2 which lead to a breakdown of the approximation over times of order $(\epsilon\omega)^{-1}$. To avoid this resonance, as in the standard procedure,[11–13] we impose the solvability condition that the right-hand side of the equation be orthogonal to the solution of the (adjoint) homogeneous equation, namely $\exp(-i\omega\hat{t})P_1$:

$$\int_0^L S[\exp(-i\omega\hat{t})P_1]\left(2i\omega\frac{dA}{d\tau}P_1-\frac{A}{\epsilon}\{\cdots\}\right)\exp(i\omega\hat{t})dx=0, \tag{30}$$

where, for brevity, we write $\{\cdots\}$ to denote the coefficient of A in (29). Multiplication by $S(x)$ before integration is necessary so that the x-operator in the left hand side of (29) be self-adjoint with the boundary conditions (24). In this way we find

$$\frac{dA}{d\tau}+\frac{\Omega}{\epsilon}A=0, \tag{31}$$

where

$$\Omega=\tfrac{1}{2}(M_D+iN_D+M_H+iN_H) \tag{32}$$

with, after an integration by parts,

$$M_D+iN_D=\frac{i}{Vp_0^2\omega}\int_0^L Sc^2\frac{f_V}{1-f_V}\left(\frac{dP_1}{dx}\right)^2 dx, \tag{33}$$

$$M_H+iN_H=i\frac{\gamma-1}{Vp_0^2\omega}\int_0^L dx\ SP_1\left[f_K\omega^2P_1-\frac{f_K-f_V}{(1-\sigma)(1-f_V)}c_p\frac{dT_w}{dx}\frac{dP_1}{dx}\right], \tag{34}$$

where c_p is the specific heat at constant pressure.

Since the f's are essentially the small parameter ϵ, and since these results have an accuracy of first order in ϵ, one might be tempted to replace $1-f_V$ simply by 1 in the denominators. While justified in principle in the limit $\epsilon\to 0$, we have found that the numerical accuracy of these results extends to significantly larger values of δ/l if the forms given above are retained.

Clearly (34) is also applicable when T_w depends slowly (i.e., on the time scale τ) on time. Integration of the amplitude equation (31) in this case is however somewhat more complicated and therefore, as already mentioned before, we limit ourselves to the simpler situation in which T_w is independent of time. In this case the solution of (31) is

$$A(\tau)=A_0\exp\left(-\Omega\frac{\tau}{\epsilon}\right)=A_0\exp(-\Omega t), \tag{35}$$

with A_0 dependent on the initial conditions, and therefore grows or decays according to the sign of M_D+M_H. The second form of solution (35) demonstrates explicitly the independence of the result from the definition of ϵ. The previous results imply the following approximation for the exact eigenfrequency $\hat{\omega}$ in Rott's equation (11):

$$\hat{\omega}\simeq\omega+i\Omega. \tag{36}$$

It is interesting to verify that (35) reduces to the standard expressions for the viscous and thermal damping of a standing wave in a hollow isothermal cylindrical tube. If we consider the case of rigid terminations at both ends, by the normalization (25), we may write

$$P_1 = \sqrt{2} p_0 \cos \frac{n\pi x}{L}. \tag{37}$$

With this expression, noting that $\omega = n\pi c/L$, and using approximation (10) for $f_{V,K}$, it is immediate to verify that, to lowest order in these quantities,

$$M_D + iN_D \simeq (1+i) \frac{\sqrt{2\nu\omega}}{r_0}, \tag{38}$$

$$M_H + iN_H \simeq (1+i)(\gamma - 1) \frac{\sqrt{2\alpha\omega}}{r_0}, \tag{39}$$

in agreement with well-known results (see, e.g., Ref. 17, p. 534).

In view of the proportionality of $\mathscr{E}$ to the A^2 shown by (26), we also see that (31) implies

$$\frac{d\mathscr{E}}{dt} = -(M_D + M_H)\mathscr{E}. \tag{40}$$

In the unstable case $M_D + M_H < 0$ and this relation gives the growth rate of the disturbance energy. In the stable case $M_D + M_H > 0$ and, in order to maintain the oscillations, one needs to supply energy externally at the rate dictated by the right hand side of (40). In this case the energy lost is in part dissipated by viscosity and thermal conduction, but in part is also the work needed to transport heat from the colder to the warmer regions as, in this case, the device behaves as a heat pump, or acoustic refrigerator.

Swift[6] defines the work flux $\dot{W}_2$ in a thermoacoustic engine. This is equivalent to the rate of growth (or decay) of the total acoustic energy in the device and, in the present notation, is therefore given by

$$\dot{W}_2 = -(M_D + M_H)\mathscr{E}. \tag{41}$$

The connection between Swift's expression for $\dot{W}_2$ and our result is best explained after the considerations of Subsection III A.

The quality factor Q is defined by

$$Q = -\frac{\omega \mathscr{E}}{\dot{W}_2}, \tag{42}$$

which, with (32) and (41), becomes

$$Q = \frac{\omega}{2\,\mathrm{Re}\,\Omega}. \tag{43}$$

This relation establishes a connection between the present study and the work of Atchley[7–9] who estimated the growth rate of the instability using an approximate calculation of $\mathscr{E}$ and $\dot{W}_2$. The present approach has the advantage of greater generality which, as will be seen in the following sections, leads to very accurate results.

III. SHORT-STACK APPROXIMATION

The asymptotic results of Sec. I can be approximated by adopting the so-called ''short-stack approximation'' (see, e.g., Ref. 6). We thus assume that the stack occupies a length much smaller than the wavelength of the standing waves so that the pressure field in the stack can be considered as constant. We take $f_{V,K} \simeq 0$ outside the stack region.

We thus write (33), approximately, as

$$M_D + iN_D \simeq \frac{i\overline{f_V}}{1-\overline{f_V}} \frac{V_S}{V} \frac{\overline{c^2}}{\omega p_0^2} \left(\frac{dP_{1S}}{dx} \right)^2. \tag{44}$$

Here $\overline{f_V}$ and $\overline{c^2}$ (or, equivalently $\overline{T_w}$) are evaluated at the mean temperature in the stack, $T_w = \frac{1}{2}(T_C + T_H)$. It is difficult on the basis of *a priori* considerations to formulate the kind of averaging that is most effective for the present purposes. We have tried several definitions, such as averaging computed by integration along the stack, but found insignificant differences. Furthermore,

$$V_S = \int_{x_{S-(1/2)L_S}}^{x_{S+(1/2)L_S}} dx\, S(x) \tag{45}$$

is the volume of the gas in the stack region extending from $x_S - \frac{1}{2}L_S$ to $x_S + \frac{1}{2}L_S$. The index S appended to P_1 denotes evaluation at the stack's midpoint x_S. In a similar way, from (34),

$$M_H + iN_H \simeq i \frac{V_S}{V} \frac{\omega}{p_0^2} \left[(\gamma - 1)\overline{f_K}(P_{1S})^2 - \frac{\overline{f_K} - \overline{f_V}}{(1-\sigma)(1-\overline{f_V})} \frac{1}{\omega^2} \overline{\frac{dc^2}{dx}} P_{1S} \frac{dP_{1S}}{dx} \right], \tag{46}$$

and, upon combining results (44) and (46),

$$M_D + M_H \simeq \frac{V_S}{V} \frac{\omega}{p_0^2} \left[Z_1 \frac{\overline{c^2}}{\omega^2} \left(\frac{dP_{1S}}{dx} \right)^2 + (\gamma - 1) Z_2 (P_{1S})^2 - Z_3 \frac{1}{\omega^2} \overline{\frac{dc^2}{dx}} P_{1S} \frac{dP_{1S}}{dx} \right], \tag{47}$$

where we have set for brevity

$$Z_1 = -\mathrm{Im}\left(\frac{\overline{f_V}}{1-\overline{f_V}} \right), \quad Z_2 = -\mathrm{Im}(\overline{f_K}), \quad Z_3 = \frac{1}{1-\sigma} \mathrm{Im}\left(\frac{\overline{f_V} - \overline{f_K}}{1-\overline{f_V}} \right). \tag{48}$$

For small diffusion penetration depths, from (10), these quantities are given by

$$Z_1 \simeq \frac{\overline{\delta_V}}{l}, \quad Z_2 \simeq \frac{1}{\sqrt{\sigma}} \frac{\overline{\delta_V}}{l}, \quad Z_3 \simeq \frac{1}{\sqrt{\sigma}(1+\sqrt{\sigma})} \frac{\overline{\delta_V}}{l}. \tag{49}$$

Use of these approximations in actual numerical calculations is not recommended. We show them to stress the dependence of the quantities Z_j on the Prandtl number and the ratio of the viscous boundary layer thicknesses to the the plate spacing.

From definitions (41) of $\dot{W}_2$ and (22) of p_1, and relation (26) we have

$$\dot{W}_2 = -\frac{V_S \omega}{\gamma p_0}\left[Z_1 \frac{\overline{c^2}}{\omega^2}\left\langle \left(\frac{\partial p_{1S}}{\partial x}\right)^2 \right\rangle + (\gamma-1) Z_2 \times \langle (p_{1S})^2 \rangle - Z_3 \frac{1}{\omega^2}\frac{\overline{dc^2}}{dx}\left\langle p_{1S}\frac{\partial p_{1S}}{\partial x}\right\rangle \right], \tag{50}$$

where the angle brackets denote time average over one cycle. In his Eq. (80) Swift[6] gives an expression for the work flux $\dot{W}_2$. It can be shown that his expression is the same as ours provided that $f_{V,K}$ in (48) are approximated by (10) and $\overline{dT_w/dx}$ is much larger than $\overline{T_w}/L$. Since usually $T_H - T_C$ is not very much smaller than T_w, while $L_S \ll L$, this latter approximation is often satisfied.

By equating (47) to zero we find a critical value of the temperature gradient that, if exceeded, leads to instability:

$$\left.\frac{dT_w}{dx}\right|_{\text{crit}} = \frac{1}{Z_3}\left[Z_2 \frac{\omega^2}{c_p}\frac{P_{1S}}{dP_{1S}/dx} + Z_1 \overline{T_w}\frac{dP_{1S}/dx}{P_{1S}}\right]. \tag{51}$$

If viscous effects are neglected, $\overline{f_V}=0$, $\sigma=0$ and this expression is readily shown to coincide with the critical temperature gradient defined in the elementary theory of thermoacoustic processes (see, e.g., Ref. 6). The minimum of $dT_w/dx|_{\text{crit}}$ occurs for

$$\frac{P_{1S}}{dP_{1S}/dx} = \frac{1}{\omega}\left[\frac{Z_1}{Z_2} c_p \overline{T_w}\right]^{1/2}, \tag{52}$$

where it has the value

$$\left.\frac{dT_w}{dx}\right|_{\text{min}} = 2\omega \frac{\sqrt{Z_1 Z_2}}{Z_3}\left(\frac{\overline{T_w}}{c_p}\right)^{1/2}. \tag{53}$$

In particular, in the inviscid case, any nonzero value of the temperature gradient will give rise to an instability if the stack is positioned at a pressure node.

To obtain further explicit results, we distinguish several types of boundary conditions.

A. Closed tube

Use of the previous formulae requires the approximate knowledge of ω and P_1 in the stack region. We calculate ω from

$$\omega^2 \simeq \left(\zeta \frac{n\pi}{L}\right)^2 \gamma R T_e, \tag{54}$$

where T_e is an effective temperature and ζ is a factor accounting for the difference between the actual and the ''effective'' length of the tube (see, e.g., Ref. 18 art. 265). We have used Rayleigh's method to estimate ζ, but found a negligible difference and therefore we set this quantity to 1 in the following. We take T_e to be the average temperature of the system

$$T_e = \frac{1}{L}\int_0^L T_w(x)\,dx. \tag{55}$$

We approximate the nth pressure eigenmode P_1 in the stack region by

$$P_1 = \sqrt{2} p_0 \cos\frac{\omega}{c_H}(L-x), \tag{56}$$

where $c_H = \sqrt{\gamma R T_H}$ and the factor $\sqrt{2}$ is suggested by the form of (37). Taking the wave number as ω/c_H rather than $n\pi/L$ is motivated by the result shown later that the optimal stack position for instability is near the hot end of the tube. We find that this choice indeed improves agreement with the exact solution as expected.

With these approximations we find from (47)

$$M_D + M_H \simeq 2\frac{V_S}{V}\omega\left\{ Z_1 \frac{\overline{T_w}}{T_H}\sin^2\left[\frac{\omega}{c_H}(L-x_S)\right] + (\gamma-1) Z_2 \cos^2\left[\frac{\omega}{c_H}(L-x_S)\right] - \frac{1}{2} Z_3 \frac{c_H}{\omega T_H}\frac{\overline{dT_w}}{dx}\sin\left[\frac{2\omega}{c_H}(L-x_S)\right]\right\}. \tag{57}$$

The first two terms are positive definite—and hence stabilizing—and correspond to viscous and thermal dissipation, respectively. The only potentially destabilizing term is the last one. If, as we assume, $dT_w/dx \geqslant 0$, it is therefore evident that, for instability to be possible, the stack must be positioned in a region where $\sin 2(\omega/c_H)(L-x_S) > 0$. In particular, for the fundamental mode for which $n=1$, the stack must be placed to the right of the tube's midpoint. In this case it is easy to see that $\overline{T_w} > T_e$.

With expression (54) for ω, the smallest critical temperature gradient (53) becomes

$$\left.\frac{dT_w}{dx}\right|_{\text{crit}} = 2\frac{n\pi T_e}{L}\frac{\sqrt{Z_1 Z_2}}{Z_3}\sqrt{(\gamma-1)\frac{\overline{T_w}}{T_e}}. \tag{58}$$

This relation shows that, for a given mean temperature gradient, only a finite number of modes can be unstable.

Expression (57) can be identically rewritten as

$$M_D + M_H \simeq \frac{V_S}{V}\omega Z_2\left[\frac{Z_1 \overline{T_w}}{Z_2 T_H} + \gamma - 1 + B\cos\left(2\frac{\omega}{c_H}(L-x_S) + \phi\right)\right], \tag{59}$$

where

$$B = \left[\left(\gamma - 1 - \frac{Z_1 \overline{T_w}}{Z_2 T_H}\right)^2 + \left(\frac{Z_3 c_H}{Z_2 \omega T_H}\frac{\overline{dT_w}}{dx}\right)^2\right]^{1/2}, \tag{60}$$

$$\sin\phi = \frac{1}{B}\frac{Z_3}{Z_2}\frac{c_H}{\omega T_H}\frac{\overline{dT_w}}{dx}. \tag{61}$$

Upon ignoring the small effect of the dependence of ω on x_S, it is evident from (59) that the instability will be greatest at the position where the cosine equals -1, from which

$$\sin\left[2\frac{\omega}{c_H}(L-x_S)\right] = \sin\phi. \tag{62}$$

It is readily verified that, if the mean pressure gradient is very small, this relation requires that the stack be positioned near a pressure node, as found before. However, in typical

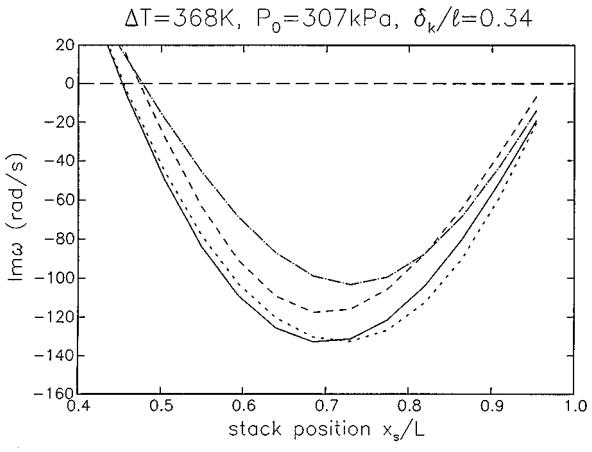

FIG. 1. Imaginary part of the eigenfrequency Im $\hat{\omega}$ as a function of the stack position x_S/L along the resonant tube. The temperature difference between the two ends of the stack is 368 K and the gas pressure 307 kPa. When the stack is positioned at the midpoint of the tube the ratio of the thermal penetration length to the spacing of the stack plates is 0.34. The solid line is the exact result from (11), the dotted line the two-time-scales result (32), the dashed line the short-stack approximation (57), and the dash-dot line Swift's result. Instability corresponds to Im $\hat{\omega}<0$.

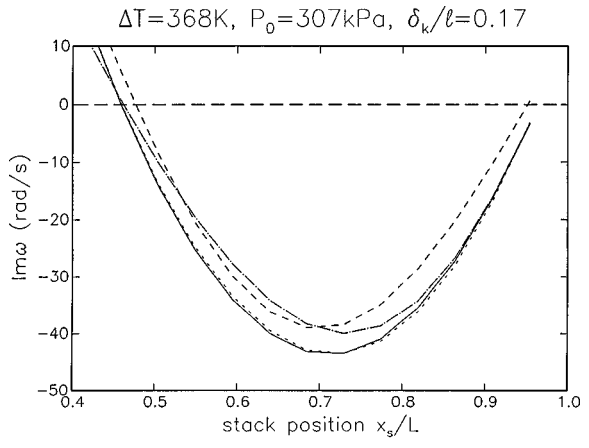

FIG. 2. Imaginary part of the eigenfrequency Im $\hat{\omega}$ as a function of the stack position x_S/L along the resonant tube. The temperature difference between the two ends of the stack is 368 K and the gas pressure 307 kPa. When the stack is positioned at the midpoint of the tube the ratio of the thermal penetration length to the spacing of the stack plates is 0.17. The solid line is the exact result from (11), the dotted line the two-time-scales result (32), the dashed line the short-stack approximation (57), and the dash-dot line Swift's result. Instability corresponds to Im $\hat{\omega}<0$.

conditions of operation of thermoacoustic devices, the stack length is much smaller than the tube length, while the temperature difference along the stack is of the order of the cold-end absolute temperature.[6] As a consequence, $\overline{dT_w/dx}$ is usually much larger than T_e/L so that, for moderate mode number n, we may approximate B and ϕ by

$$B \simeq \frac{Z_3}{Z_2}\frac{c_H}{\omega T_H}\overline{\frac{dT_w}{dx}}, \quad \sin\phi \simeq 1. \tag{63}$$

With these approximations, the optimal position of the stack to destabilize the nth mode is very nearly $\sin 2(\omega/c_H)(L-x_S)=1$, i.e., $x_S/L=1-(k+1/4)c_H/(nc_e)$, with k an integer subject to the only restrictions that $0\leqslant x_S/L\leqslant 1$. In particular, for the fundamental mode $n=1$, k must be taken as 0, so that

$$\frac{x_S}{L}=1-\frac{1}{4}\sqrt{\frac{T_H}{T_e}}. \tag{64}$$

In the elementary theory of the thermoacoustic instability, the optimal stack position is found to be at the three-quarter point $x_S=\frac{3}{4}L$, i.e., one-eighth of a wavelength from the hot end (Ref. 6; recall that here distances are measured from the cold-end of the tube). Since $T_H>T_e$, our result (64) shows that the optimal stack position is actually slightly displaced further away from the hot end of the tube, in agreement with the exact results shown in Figs. 1 and 2. It should be remarked that this conclusion only applies under the condition that $|dT_w/dx| \gg T_e/L$ and therefore it can lead to erroneous conclusions when $|dT_w/dx|$ is small.

As the order n of the mode increases, ω also increases and the constant B given by (63) accordingly decreases. Thus higher-order modes are found to be always less unstable than the fundamental one.

B. Tube open at one end

For a tube open at the cold end $x=0$ and rigidly terminated at $x=L$, we approximate the nth eigenfrequency by

$$\omega^2 \simeq \left[\left(n+\frac{1}{2}\right)\frac{\pi}{L}\right]^2 \gamma R T_e, \tag{65}$$

where the average temperature T_e is defined as before by (55). The corresponding eigenmode P_1 is taken as

$$P_1=\sqrt{2}p_0 \sin\frac{\omega}{c_C}x, \tag{66}$$

where $c_C=\sqrt{\gamma R T_C}$. Unlike the previous case, here we use ω/c_C for the wave number since the optimal stack position for instability will be found to be close to the cold end. Proceeding as before, we find

$$M_D+M_H \simeq 2\frac{V_S}{V}\omega\left[Z_1\frac{\overline{T_w}}{T_C}\sin^2\left(\frac{\omega}{c_C}x_S\right) + (\gamma-1)Z_2\cos^2\left(\frac{\omega}{c_C}x_S\right) - \frac{1}{2}Z_3\frac{c_C}{\omega T_C}\overline{\frac{dT_w}{dx}}\sin^2\left(\frac{\omega}{c_C}x_S\right)\right]. \tag{67}$$

With (65), the critical gradient (53) is

$$\left.\frac{dT_w}{dx}\right|_{\text{crit}} = 2\left(n+\frac{1}{2}\right)\frac{\pi T_e}{L}\frac{\sqrt{Z_1 Z_2}}{Z_3}\sqrt{(\gamma-1)\frac{\overline{T_w}}{T_e}}. \tag{68}$$

When $|\overline{dT_w/dx}| \gg T_e/L$ the maximum instability occurs approximately at $x_S/L=\frac{1}{2}[(4k+1)/(2n+1)](c_C/c_e)$, where $c_e=\sqrt{\gamma R T_e}$. For the lowest mode $n=0$, $k=0$ and $x_S=\frac{1}{2}L(c_C/c_e)$. This result is easily understood on the basis of the previous one as the present situation is similar to a tube of length $2L$ closed at both ends.

The case of a tube closed at the cold end and open at the other one is contained in the preceding formulae if dT_w/dx is taken to be negative. The critical gradient is the negative of (68). Again with the hypothesis that $|dT_w/dx| \gg T_e/L$, the maximum instability occurs approximately at $x_S/L = \frac{1}{2}(4k+3)/(2n+1)$. For the lowest mode $n=0$, there is no integer k such that $x_S/L \leqslant 1$. The instability condition cannot be therefore satisfied for the lowest mode of a tube open at the hot end.

C. Both ends open

For a tube open at both ends, with the cold end at $x=0$, the nth eigenfrequency is approximately given by (54). The same relations (67) and (68) of the previous case apply. The condition for instability is again given by (58). When $|\overline{dT_w/dx}| \gg T_e/L$ the maximum instability occurs for $x_S/L = \frac{1}{4}[(4k+1)/n](c_C/c_e)$, approximately. For the fundamental mode $n=1$ we thus have $k=0$ and $x_S = \frac{1}{4}(c_C/c_e)L$.

IV. COMPARISON WITH EXACT THEORY

We compare here the results of the multiple-time-scales calculation and the short stack approximation with those obtained from the exact equation (11) for some typical parameter values.

The geometry that we simulate is that of the experiments of Atchley[7,8] in which the tube length was 99.87 cm, its radius 3.82 cm, and the stack length $L_S = 3.5$ cm. The combined cross-sectional area of the stack plates was 3.1 cm^2, i.e., 27% of the entire cross section. We have calculated the exact eigenvalue $\hat{\omega}$ both accounting for, and neglecting, the blockage effect of the plates. As the differences between the two cases are very small, in the results shown below we neglect blockage for simplicity.

Of course, our purpose here is not to compare Rott's theory or our approximations with the data, a task that has already been carried out, e.g., by Atchley himself and others,[7–9,19,10] but to validate the asymptotic results against the exact ones.

The gas used in the experiment was helium and accordingly we take $\gamma = 5/3$, $\sigma = 0.71$, $c_p = 5.2$ kJ/kg K. Over the temperature range of interest here, from 300 K to 700 K, we fit thermal conductivity data[20] by a linear function of temperature as $k = 0.151 + 3.228 \times 10^{-4}(T-300)$, with k in W/m K and T in K, which provides a better fit than a power law. We have included this effect in our calculation as the value of k determines the boundary layer thickness, and therefore the heat transfer parameters. The measured temperature was approximately constant and equal to its cold and hot values to the left and right of the stack respectively, and linear in the stack and therefore we take $T = T_C$ for $0 \leqslant x \leqslant x_S - \frac{1}{2}L_S$, $T = T_H$ for $x_S + \frac{1}{2}L_S \leqslant x \leqslant L$, and

$$T = T_C + \frac{x - (x_S - \frac{1}{2}L_S)}{L_S}(T_H - T_C), \tag{69}$$

for $x_S - \frac{1}{2}L_S < x < x_S + \frac{1}{2}L_S$. Here x_S denotes the position of the midpoint of the stack.

To solve Eq. (11) numerically we multiply by S and discretize by centered differences on an equispaced grid. This procedure requires the values of $(1-f_V)S$ at the half-integer nodes which are calculated as simple arithmetic averages. Typically 2000 cells were used along the tube length, with approximately 100 in the stack region. The eigenvalues were searched by the inverse iteration method.[21] The same method was used to calculate the eigenvalues and eigenfunctions of the first-order approximation (21). The integrations necessary to calculate Ω in Eqs. (33) and (34) were effected by the trapezoidal rule. In order to avoid introducing an additional parameter—the radius of the tube—we have taken f_V and f_K to vanish outside the stack region.

As the operation of a thermoacoustic prime mover is critically dependent on the imaginary part of the eigenfrequency, we focus on this quantity. In Figs. 1 and 2 we show Im $\hat{\omega}$ as a function of the stack position x_S/L normalized by the tube length. These figures are for an undisturbed pressure of 307 kPa, with a temperature difference of 368 K along the stack. The choice of this particular case is suggested by the experimental conditions of Atchley *et al.*[9,22] The frequency Re $\hat{\omega}/2\pi$ of the fundamental mode changes from about 505 Hz to 590 Hz as the stack is moved from the hot to the middle of the tube. Within about 10%, these values are well predicted by the formula (54) with $n=1$, $\zeta=1$. Since the thermal penetration depth depends on frequency, the ratio $\overline{\delta_K}/l$ is also a function of the stack's position. When the stack is in the middle of the tube this ratio has the value 0.34 in Fig. 1 and 0.17 in Fig. 2. As the stack is moved toward the hot end, the frequency decreases and the penetration depth correspondingly increases to 0.37 for Fig. 1 and 0.19 for Fig. 2.

In Figs. 1 and 2 the solid lines mark the results from the solution of the exact Rott equation (11), the dotted lines are the two-time-scales approximation (32), the dashed lines are the short-stack approximation (57), and the dash-dot lines are the results obtained from Eq. (80) in Swift[6] according to (41). The zero is marked by the horizontal line; a negative value of Im $\hat{\omega}$ implies instability, and a positive one stability. Agreement between the two-times approximation (32) and the exact solution is excellent even at the relatively large value of $\overline{\delta_K}/l$ of Fig. 1. The difference is hardly noticeable at the smaller value of Fig. 2, and practically disappears for even larger gaps. The short-stack approximation (57) is not as accurate, but the error is less than about 15% even in the worst case. Swift's result is good for the wider gap case of Fig. 2 but, as Fig. 1 shows, it rapidly deteriorates as the gap width decreases. It should be noted that, in plotting Swift's result, the values of pressure and velocity appearing in Swift's formula have been obtained from the exact solution of Rott's equation.

Another important quantity is the critical temperature gradient, which is shown in Figs. 3 to 5 as a function of $\overline{\delta_K}/l$ for stack positions at $x_S/L = 0.594$, 0.729, 0.864, respectively. Here the geometry and conditions are as in the previous figures except for the hot temperature T_H which is evaluated as follows. In the case of the exact Rott solution T_H is adjusted so as to achieve marginal stability conditions (i.e., Im $\hat{\omega}=0$) with a fixed stack length L_S, after which the critical temperature gradient is calculated as $(T_H - T_C)/L_S$. (Recall that the stack temperature is prescribed to be linear in

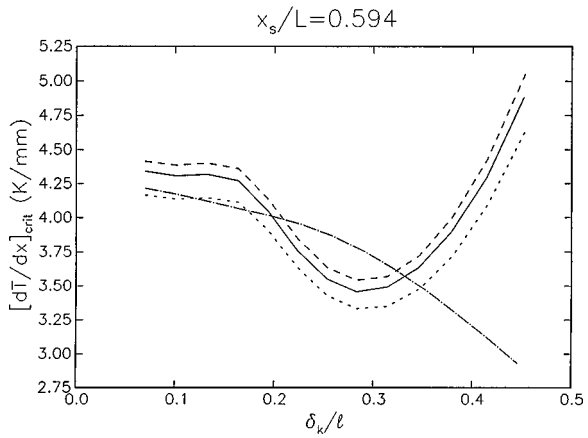

FIG. 3. Critical temperature gradient as a function of the ratio of the thermal penetration length δ_K to the gap width l for a stack positioned at $x_S/L = 0.594$, i.e., near the midpoint of the tube. The solid line is the exact Rott result, the dotted line the short-stack approximation (51) with P_1 approximated by the hot-temperature wave function (56), and the dashed line by the cold-temperature wave function (66). The dash-dot line is the result found by setting Swift's (Ref. 6) Eq. (80) to 0. The large discrepancy is principally due to the use of the approximation (10) for the $f_{V,K}$'s in (48).

this work.) These results are shown by the solid lines in the figures. The short-stack approximation to the critical temperature gradient has been calculated from (51) which, with $dT_w/dx=(T_H-T_C)/L_S$, can be regarded as an equation for T_H. The dotted line shows this result with P_1 approximated by (56), while the dashed line is found from a corresponding approximation, (66), based on the cold-temperature wave number. For the two positions closest to the hot end of the tube (Figs. 4 and 5) most of the tube is occupied by gas at the cold temperature and use of the second form of the eigenfunction gives a somewhat better result. When the stack is positioned near the midpoint of the tube (Fig. 3), on the other hand, both alternatives give a comparable error that can be reduced by using the average of the two approximations to P_1 (not shown). We have repeated these calculations using

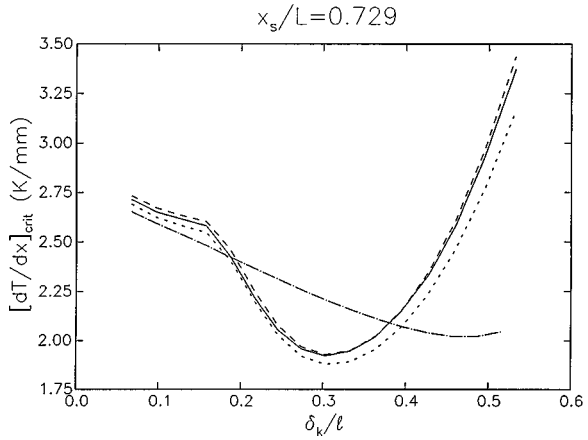

FIG. 4. Critical temperature gradient as a function of the ratio of the thermal penetration length δ_K to the gap width l for a stack positioned at $x_S/L = 0.729$. The solid line is the exact Rott result, the dotted line the short-stack approximation (51) with P_1 approximated by the hot-temperature wave function (56), and the dashed line by the cold-temperature wave function (66). The dash-dot line is the result found by setting Swift's (Ref. 6) Eq. (80) to 0. The large discrepancy is principally due to the use of the approximation (10) for the $f_{V,K}$'s in (48).

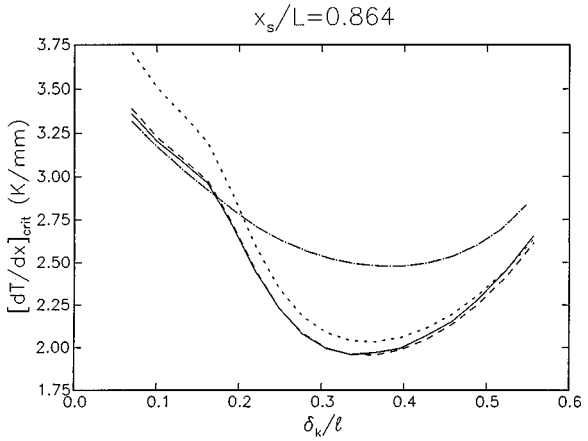

FIG. 5. Critical temperature gradient as a function of the ratio of the thermal penetration length δ_K to the gap width l for a stack positioned at $x_S/L = 0.864$. The solid line is the exact Rott result, the dotted line the short-stack approximation (51) with P_1 approximated by the hot-temperature wave function (56), and the dashed line by the cold-temperature wave function (66). The dash-dot line is the result found by setting Swift's (Ref. 6) Eq. (80) to 0. The large discrepancy is principally due to the use of the approximation (10) for the $f_{V,K}$'s in (48).

the exact two-time-scale expression (51) with P_1 found numerically from (23). When the stack is positioned near the tube's midpoint the error is about 1%. When however the stack is moved toward the hot end, this result is comparable to that obtained by the short-stack approximation with the cold-temperature wave number.

In Figs. 3 to 5 the dash-dot lines show the result obtained by setting Swift's expression for $\dot{W}_2$ to 0. The error incurred in the approximation of $f_{V,K}$ by (10) is seen to lead to a substantial discrepancy with the exact results. Our result would show a comparable error if the same approximations for $f_{V,K}$ were used.

V. CONCLUSIONS

By exploiting the difference between the time scale for the development of the thermoacoustic instability and the period of standing waves in a resonant tube, we have developed a time-domain description of the instability and approximate formulae for its growth rate. We have carried out a multiple-time-scales expansion to first order and we have given simplified formulae exploiting the short-stack approximation. In addition to closed tubes, we have also considered tubes open at either or both ends. Results for modes higher than the fundamental one have also been presented.

The exact perturbation results are very close to the theoretical prediction of the full Rott equation. In practice, their evaluation requires the solution of the eigenvalue problem (21) that is self-adjoint and has therefore real eigenvalues. Accordingly, numerically the problem is more tractable than Rott's equation. Even this rather modest computational task can be avoided—at the price of an error of a few percent—by adopting the short-stack approximation discussed in Sec. III.

Another significant result of the present study is an accurate (and numerically manageable) approximation for the critical temperature gradient including viscosity, heat trans-

fer, and cross-sectional area changes. As Figs. 3 to 5 show, the present expression is significantly more accurate than others available in the literature.

As a final point, the approximate result (40) for the rate of energy loss of a thermoacoustic device below the instability threshold enables one to readily calculate the minimum power required to maintain a certain temperature difference across the stack, i.e., to operate the device as a refrigerator.

Although we have only considered a particular type of thermoacoustic devices, in which the heated region contains the so-called stack, the same method can be applied to other configurations. The present results imply that good accuracy may be expected as a result of this approach.

ACKNOWLEDGMENTS

The authors would like to express their gratitude to one of the referees useful suggestions. They are also grateful to the Office of Naval Research for the support of this work.

[1] N. Rott, ''Damped and thermally driven acoustic oscillations in wide and narrow tubes,'' Z. Angew. Math. Phys. **20**, 230–243 (1969).
[2] N. Rott, ''Thermally driven acoustic oscillations, Part IV: Tubes with variable cross section,'' Z. Angew. Math. Phys. **27**, 197–224 (1976).
[3] N. Rott, ''Thermoacoustics,'' Adv. Appl. Mech. **20**, 135–175 (1980).
[4] N. Rott, ''Thermally driven acoustic oscillations, Part VI: Excitation and power,'' Z. Angew. Math. Phys. **34**, 609–626 (1983).
[5] J. Wheatley, ''Intrinsically irreversible or natural heat engines,'' in *Frontiers in Physical Acoustics*, edited by D. Sette (North-Holland, New York, 1986), pp. 35–475.
[6] G. W. Swift, ''Thermoacoustic engines,'' J. Acoust. Soc. Am. **84**, 1145–1180 (1988).
[7] A. A. Atchley, ''Standing wave analysis of a thermoacoustic prime mover below onset of self-oscillation,'' J. Acoust. Soc. Am. **92**, 2907–2914 (1992).
[8] A. A. Atchley, ''Analysis of the initial build-up of oscillations in a thermoacoustic prime mover,'' J. Acoust. Soc. Am. **95**, 1661–1664 (1994).
[9] A. A. Atchley, H. E. Bass, T. J. Hofler, and H.-T. Lin, ''Study of a thermoacoustic prime mover below onset of self-oscillation,'' J. Acoust. Soc. Am. **91**, 734–743 (1992).
[10] M. Watanabe, A. Prosperetti, and H. Yuan, ''A simplified model for linear and nonlinear processes in thermoacoustic prime movers. Part I. model and linear theory,'' J. Acoust. Soc. Am. **102**, 3484–3496 (1997).
[11] J. Kevorkian and J. D. Cole, *Perturbation Methods in Applied Mathematics* (Springer-Verlag, New York, 1996), 2nd ed., Sec. 3.2.
[12] J. A. Murdock, *Perturbations* (Wiley, New York, 1991), pp. 227–233.
[13] E. J. Hinch, *Perturbation Methods* (Cambridge U.P., Cambridge, 1991), pp. 116–126.
[14] P. M. Morse and H. Feshbach, *Methods of Theoretical Physics* (McGraw-Hill, New York, 1953).
[15] A. W. Naylor and G. R. Sell, *Linear Operator Theory in Engineering and Science* (Springer-Verlag, New York, 1982), 2nd ed.
[16] L. Landau and E. M. Lifshitz, *Fluid Mechanics* (Pergamon, Oxford, 1959).
[17] A. D. Pierce, *Acoustics* (American Institute of Physics, Woodbury, NY, 1989), 2nd ed.
[18] Lord Rayleigh, *The Theory of Sound* (Macmillan, London, 1896, Reprinted by Dover, 1945).
[19] A. A. Atchley and F. M. Kuo, ''Stability curves for a thermoacoustic prime mover,'' J. Acoust. Soc. Am. **95**, 1401–1404 (1994).
[20] N. B. Vargaftik, *Handbook of Physical Properties of Liquids and Gases* (Wiley, New York, 1975).
[21] W. H. Press, W. T. Vetterling, S. A. Teukolsky, and B. P. Flannery, *Numerical Recipes in FORTRAN* (Cambridge U.P., Cambridge, 1992), 2nd ed.
[22] A. A. Atchley, H. E. Bass, and T. J. Hofler, ''Development of nonlinear waves in a thermoacoustic prime mover,'' in *Frontiers in Nonlinear Acoustics*, edited by M. F. Hamilton and D. T. Blackstock (Elsevier, New York, 1990), pp. 603–608.